

Top-quark pair-production with one jet and parton showering at hadron colliders

Simone Alioli¹, Juan Fuster², Adrian Irles², Sven-Olaf Moch³, Peter Uwer⁴, Marcel Vos²

¹LBNL & UC Berkeley, 1 Cyclotron Road, Berkeley, CA 94720, USA

³IFIC, Universitat de Valencia – CSIC, Catedrático Jose Beltrán 2, E-46980 Paterna, Spain

³DESY, Platanenalle 6, D-15738 Zeuthen, Germany

⁴Humboldt-Universität, Newtonstraße 15, D-12489 Berlin, Germany

DOI: will be assigned

We present heavy-flavor production in association with one jet in hadronic collisions matched to parton shower Monte Carlo predictions at next-to-leading order QCD with account of top-quark decays and spin correlations. We use the POWHEG BOX for the interface to the parton shower programs PYTHIA or HERWIG. Phenomenological studies for the LHC and the Tevatron are presented with particular emphasis on the inclusion of spin-correlation effects in top decay and the impact of the parton shower on the top-quark charge asymmetries. As a novel application of the present calculation the measurement of the top-quark mass is discussed.

1 Introduction

The Large Hadron Collider (LHC) and the Tevatron provide an experimental environment allowing for top-quark measurements with percent level accuracy. Precise measurements for top-quark production demand theoretical predictions with comparable precision. This requires the knowledge of the hard scattering process beyond the leading order (LO) in perturbation theory. Furthermore, for the direct comparison with experimental data, fully exclusive events are needed, that take into account all-order logarithmic enhancements of soft and collinear regions of phase space and hadronization effects by means of Shower Monte Carlo (SMC) programs. Both approaches can be combined systematically by merging NLO computations with parton showers, in the MC@NLO [1] or POWHEG [2] approach.

2 $t\bar{t}$ + 1-jet hadroproduction in POWHEG

In the following we concentrate on the recent implementation of the $t\bar{t}$ + 1-jet hadroproduction in the POWHEG approach, presented in Ref. [3]. A large fraction of the inclusive $t\bar{t}$ production does indeed actually contain events with one or even more additional jets. Furthermore, due to the larger phase space available, the relative importance of data samples with $t\bar{t}$ +jets is larger at the LHC with respect to the Tevatron, increasing the need of an accurate theoretical description of this process. Top-quark pair-production associated with jets is also an important background to Higgs boson production in vector boson fusion and for many signals of new

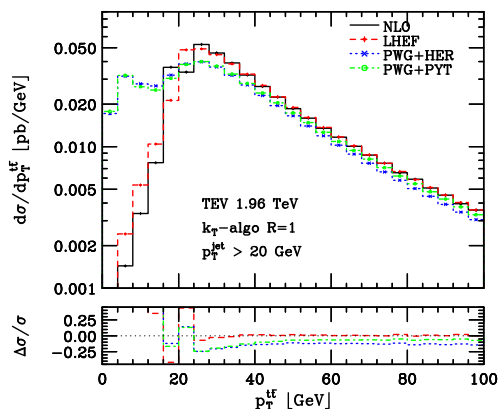


Figure 1: Differential cross section as a function of the $t\bar{t}$ -pair transverse momentum at the Tevatron ($\sqrt{s} = 1.96$ TeV)

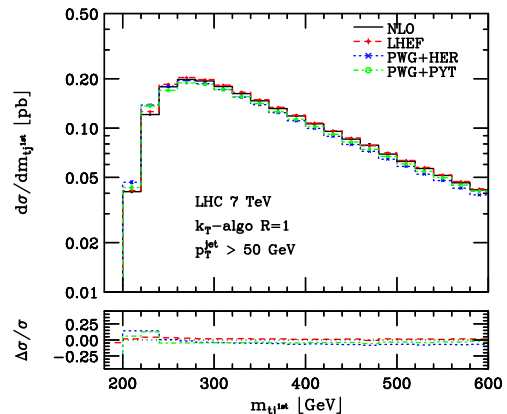


Figure 2: Differential cross section as a function of the (tj_1) invariant mass at the LHC ($\sqrt{s} = 7$ TeV)

physics. The implementation reported here is based on the NLO QCD corrections evaluated in Ref. [4, 5], merged with HERWIG [6] and PYTHIA [7] SMC programs, using the POWHEG BOX [8].

We present results for both Tevatron and LHC colliders, having assumed a jet reconstruction cut in the analysis of $p_T > 20$ GeV and 50 GeV, respectively. We have used the inclusive- k_T jet algorithm with $R = 1$ and the E_T -recombination scheme. Renormalization and factorization scales have been set to $\mu_R = \mu_F = m_t = 174$ GeV, we have used the PDF set CTEQ6M [9], and we have not imposed any extra acceptance cut, other than those necessary to define the hard jet. In Fig. 1 we show the differential cross section as a function of the transverse momentum of the $t\bar{t}$ -pair at the Tevatron, while in Fig. 2 we plot the invariant mass of the system made by the top-quark and the hardest jet at the 7 TeV LHC. The different curves appearing on each plot refer respectively to the fixed order results (NLO), to the results after the first emission has been performed by POWHEG (LHEF) and to the fully showered events, with HERWIG (PWG+HER) or PYTHIA (PWG+PYT) showers. Shower effects are visible in the low- $p_T^{t\bar{t}}$ region, while more inclusive observables like the invariant mass of the system made by the top-quark and the hardest jet, $m_{(tj_1)}$, are basically unaffected by the shower.

3 Spin correlations in top-quark decays

In our implementation we have also included the spin-correlations. In doing so, we have neglected off-shell effects and non-resonant production mechanisms. We proceeded by first generating events with stable top-quarks (un-decayed events) through the usual POWHEG machinery and then generating the decay products according to the matrix element for the full production and decay process (decayed events), following Ref. [10]. In our study we always assumed the double-leptonic top-quark decay channel $t \rightarrow W^+ b \rightarrow \ell^+ \nu b$. In Fig. 3 we draw the differential distribution $\frac{1}{\sigma} \frac{d^2\sigma}{d\cos\theta_1 d\cos\theta_2}$ after the HERWIG shower, at the Tevatron collider, where the angles θ_1 and θ_2 between the directions of flight of the leptons coming from the decayed top-quark in the t (\bar{t}) rest frame and the beam axis can be interpreted in the context of spin correlations as the quantization axis for the (anti-)top-quark spin. No extra acceptance cut is imposed on the

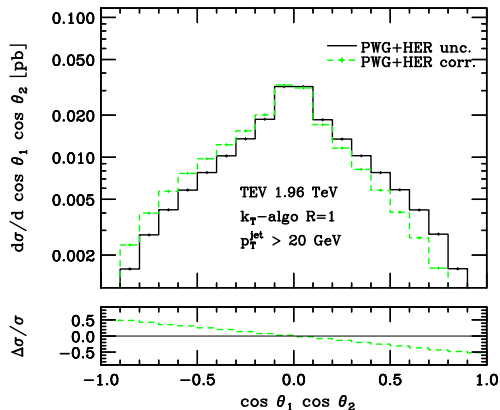


Figure 3: Effect of the inclusion of spin correlations when interfacing to HERWIG.

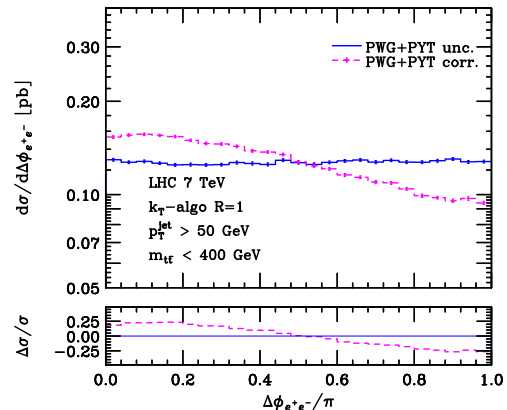


Figure 4: Effect of the inclusion of spin correlations when interfacing to PYTHIA.

leptons. In Fig. 4 we show instead the differential cross section as a function of the azimuthal distance between the two leptons coming from the top-quarks decays, for the LHC collider configuration and after the PYTHIA shower. An extra cut $m_{t\bar{t}} < 400$ GeV has been imposed here to enhance the effect. A similar observable has recently been used in $t\bar{t}$ -production to observe spin-correlations [11]. The plots in Fig. 4 clearly demonstrate the differences between spin-correlated results and those obtained by letting the respective SMC program performing uncorrelated top-quark decays.

4 Asymmetries

We have also investigated the $t\bar{t}$ charge asymmetry in presence of a hard jet, finding that the inclusion of the parton shower changes significantly the fixed-order predictions in the low $p_T^{t\bar{t}}$ region, where shower effects are known to be large. Away from this region the parton shower leads only to a marginal change of the charge asymmetry binned in $p_T^{t\bar{t}}$. This quantity is now available at NLO accuracy, supplemented by the shower. For more details and for complete tables including results obtained with different cuts and at various stages of the simulation, we refer to Ref. [3].

5 Top-quark mass measurement

As a novel application the differential cross section for $t\bar{t} + 1$ -jet production can be used for a determination of the top-quark mass. To that end, we consider the differential $t\bar{t} + 1$ -jet rate,

$$\frac{dn_3}{d\rho_s}(m_{top}^p, \mu, \rho_s) = \frac{1}{\sigma_{t\bar{t}j}} \frac{d\sigma_{t\bar{t}j}}{d\rho_s}(m_{top}^p, \mu, \rho_s), \quad (1)$$

where $\sigma_{t\bar{t}j}$ denotes the cross section for the process $pp \rightarrow t\bar{t} + 1\text{-jet} + X$. The variable ρ_s is defined as $\rho_s = \frac{2 \cdot m_0}{\sqrt{s_{t\bar{t}j}}}$ with $m_0 = 170$ GeV and $s_{t\bar{t}j}$ is the invariant mass squared of the final state. In Fig. 5 a clear separation between the distributions for different top-quark masses is observed except in the region of $0.55 < \rho_s < 0.62$ where the curves cross due to the normalization of

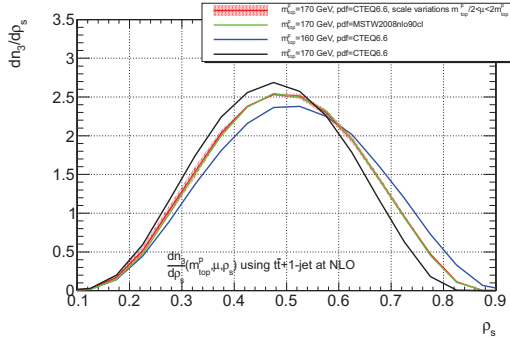


Figure 5: $dn_3/d\rho_s(m_{top}^p, \mu)$ calculated at NLO for different masses $m_{top}^p = 160, 170$ and 180 GeV. For $m_{top}^p = 170$ GeV the scale uncertainty is shown and two PDF sets [13, 14] for comparison.

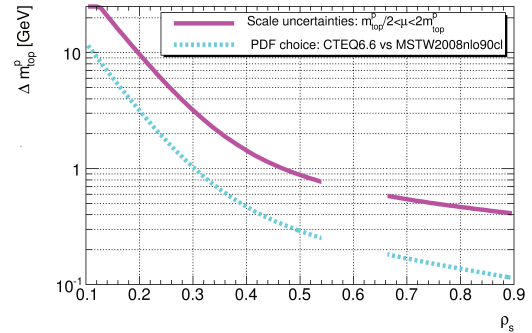


Figure 6: Sensitivity on value of the top-quark mass (for $m_{top}^p = 170$ GeV) along with scale uncertainty (magenta solid line) and effect of PDF choice [13, 14]. The crossing region is excluded.

$\frac{dn_3}{d\rho_s}(m_{top}^p, \mu, \rho_s)$. As a consequence a decrease of sensitivity is observed in the crossing region. The approach of Eq. (1) nicely complements top-quark mass measurements from the $t\bar{t}$ total cross section, see Ref. [12] for the first measurement of the \overline{MS} mass. The impact of the conventionally estimated scale variation (solid line) and the PDF choice (dashed line) on the top mass value (for $m_{top}^p = 170$ GeV) is displayed in Fig. 6. It demonstrates that a theoretical uncertainty of 500–600 MeV can be reached with a mass measurement in the interval $\rho_s > 0.62$ based on the scale uncertainty and the dependence on the PDF choice. Additional sources of systematic uncertainties have been investigated and have led to error estimates below 1 GeV. The crossing region is again excluded due to the vanishing sensitivity. The curves in Fig. 6 have been obtained assuming a linear dependence of n_3 on the top-quark mass for intervals of $\Delta m_{top}^p = 5$ GeV.

References

- [1] S. Frixione and B. R. Webber. JHEP **0206** (2002) 029, arXiv:hep-ph/0204244 .
- [2] P. Nason. JHEP **0411** (2004) 040, arXiv:hep-ph/0409146 .
- [3] S. Alioli, S. Moch, and P. Uwer. JHEP **1201** (2012) 137, arXiv:1110.5251.
- [4] S. Dittmaier, P. Uwer, and S. Weinzierl. Phys.Rev.Lett. **98** (2007) 262002, arXiv:hep-ph/0703120 .
- [5] S. Dittmaier, P. Uwer, and S. Weinzierl. Eur.Phys.J. **C59** (2009) 625–646, arXiv:0810.0452.
- [6] G. Corcella *et al.* JHEP **0101** (2001) 010, arXiv:hep-ph/0011363 .
- [7] T. Sjostrand, S. Mrenna, and P. Z. Skands. JHEP **0605** (2006) 026, arXiv:hep-ph/0603175 .
- [8] S. Alioli *et al.* JHEP **1006** (2010) 043, arXiv:1002.2581.
- [9] J. Pumplin *et al.* JHEP **0207** (2002) 012, arXiv:hep-ph/0201195 .
- [10] S. Frixione *et al.* JHEP **0704** (2007) 081, arXiv:hep-ph/0702198 .
- [11] G. Aad *et al.* Phys.Rev.Lett. **108** (2012) 212001, arXiv:1203.4081 [hep-ex].
- [12] U. Langenfeld, S. Moch, and P. Uwer. Phys.Rev. **D80** (2009) 054009, arXiv:0906.5273.
- [13] P. M. Nadolsky *et al.* Phys.Rev. **D78** (2008) 013004, arXiv:0802.0007.
- [14] A. Martin *et al.* Eur.Phys.J. **C63** (2009) 189–285, arXiv:0901.0002.